

Footprints of ALP

in PTA and JWST Observations

Shu-Yuan Guo (Yantai University)

Collaborate with

Maxim Khlopov, Xuewen Liu, Lei Wu,
Yongcheng Wu and Bin Zhu

arXiv:2306.17022

Contents

- Introduction to the ALP model and Domain Walls
- Generation of the stochastic gravitational wave background
- Implication on JWST and axion detections
- Conclusion

The ALP Model and Domain Walls

The ALP Model

- A typical potential term in ALP model

$$V = \frac{\lambda}{2}(\Psi^*\Psi - f_a^2)^2 + \Lambda^4(1 - \cos \theta)$$

The ALP Model

- A typical potential term in ALP model

$$V = \frac{\lambda}{2}(\Psi^*\Psi - f_a^2)^2 + \Lambda^4(1 - \cos \theta)$$

$$\Psi_{vac} = f_a \exp(i\theta) \text{—degenerate vacua}$$

The ALP Model

- A typical potential term in ALP model

$$V = \frac{\lambda}{2}(\Psi^*\Psi - f_a^2)^2 + \Lambda^4(1 - \cos \theta)$$

$$\Psi_{vac} = f_a \exp(i\theta) \text{—degenerate vacua}$$



$$\theta_{vac} = 0, 2\pi, 4\pi, \dots \text{—discrete set of vacua}$$

The ALP Model

- A typical potential term in ALP model

$$V = \frac{\lambda}{2}(\Psi^*\Psi - f_a^2)^2 + \Lambda^4(1 - \cos \theta)$$

- Symmetry breaking results in pNG boson $\phi = f_a \theta$ and $m_\phi = \Lambda^2/f_a$.

The ALP Model

- A typical potential term in ALP model

$$V = \frac{\lambda}{2}(\Psi^*\Psi - f_a^2)^2 + \Lambda^4(1 - \cos \theta)$$

- Symmetry breaking results in pNG boson $\phi = f_a \theta$ and $m_\phi = \Lambda^2/f_a$.
- Domain walls form between true vacua when the fluctuation $\delta\theta$ crosses π .

The ALP Model

- A typical potential term in ALP model

$$V = \frac{\lambda}{2}(\Psi^*\Psi - f_a^2)^2 + \Lambda^4(1 - \cos \theta)$$

- Symmetry breaking results in pNG boson $\phi = f_a\theta$ and $m_\phi = \Lambda^2/f_a$.
- Domain walls form between true vacua when the fluctuation $\delta\theta$ crosses π .
- The fate of domain walls depend on their size, they could either collapse into PBHs, or escape into baby universe and leaving wormholes. Both of them radiate their energy through GWs.

Generation of SGWB

Generation of SGWB

- Fractional energy density of gravitational waves:

Generation of SGWB

- Fractional energy density of gravitational waves:

$$\Omega_{\text{gw}}(\ln f) = \frac{8\pi G}{3H_0^2} f \rho_{\text{gw}}(t_0, f)$$

Generation of SGWB

- Fractional energy density of gravitational waves:

$$\Omega_{\text{gw}}(\ln f) = \frac{8\pi G}{3H_0^2} f \rho_{\text{gw}}(t_0, f)$$

$$\rho_{\text{gw}}(t_0, f) = \int_{t_{\text{sw}}}^{t_0} \frac{dt}{(1+z(t))^4} P_{\text{gw}}(t, f') \frac{\partial f'}{\partial f}$$

(energy density in comoving volume)

Generation of SGWB

- Fractional energy density of gravitational waves:

$$\Omega_{\text{gw}}(\ln f) = \frac{8\pi G}{3H_0^2} f \rho_{\text{gw}}(t_0, f)$$

$$\rho_{\text{gw}}(t_0, f) = \int_{t_{\text{sw}}}^{t_0} \frac{dt}{(1+z(t))^4} P_{\text{gw}}(t, f') \frac{\partial f'}{\partial f}$$

(energy density in comoving volume)

$$P_{\text{gw}}(t, f') = \frac{dn(t, f')}{df'} P_{\text{gw},i}$$

(GWs energy power)

Generation of SGWB

- For PBH

$$P_{\text{gw},i}^{\text{PBH}} \approx \frac{G}{C_2} \frac{\sigma^2}{f'^2}$$

Phys.Rev.D **104** (2021) 043005

Generation of SGWB

- For PBH

$$P_{\text{gw},i}^{\text{PBH}} \approx \frac{G}{C_2} \frac{\sigma^2}{f^2}$$

Phys.Rev.D **104** (2021) 043005

$$\sigma = 4\Lambda^2 f_a$$

Generation of SGWB

- For PBH

$$P_{\text{gw},i}^{\text{PBH}} \approx \frac{G}{C_2} \frac{\sigma^2}{f'^2}$$

Phys.Rev.D **104** (2021) 043005

$$\sigma = 4\Lambda^2 f_a$$

leads to the fractional energy density as

$$\Omega_{\text{gw}}^{\text{PBH}}(\ln f) = \frac{32\sqrt{2}\pi}{21C_2} \frac{\Omega_r^{1/4}}{H_0^{3/2}} \Gamma_s (G\sigma)^2 f^{-1/2}$$

Generation of SGWB

- For Wormhole

$$P_{\text{gw},i}^{\text{WH}} \approx \frac{\kappa^2}{4C_2G}$$

Phys.Rev.D **104** (2021) 043005

Generation of SGWB

- For Wormhole

$$P_{\text{gw},i}^{\text{WH}} \approx \frac{\kappa^2}{4C_2 G}$$

Phys.Rev.D **104** (2021) 043005

κ —fraction of mass set in GWs

Generation of SGWB

- For Wormhole

$$P_{\text{gw},i}^{\text{WH}} \approx \frac{\kappa^2}{4C_2 G}$$

Phys.Rev.D **104** (2021) 043005

κ —fraction of mass set in GWs

leads to the fractional energy density as

$$\Omega_{\text{gw}}^{\text{WH}}(\ln f) = \frac{8\sqrt{2}\pi}{9C_2} \frac{\Omega_r^{1/4}}{H_0^{3/2}} \kappa^2 \Gamma_s f^{3/2}$$

Generation of SGWB

- The generated SGWB:

$$\Omega_{\text{GW}}(f) = \frac{8\pi\sqrt{2}\Omega_r^{1/4}}{3C_2H_0^{3/2}}\Gamma_s\left(\frac{1}{3}\kappa^2f^{3/2} + \frac{4}{7}(G\sigma)^2f^{-1/2}\right)$$

Generation of SGWB

- The generated SGWB:

$$\Omega_{\text{GW}}(f) = \frac{8\pi\sqrt{2}\Omega_r^{1/4}}{3C_2H_0^{3/2}}\Gamma_s\left(\frac{1}{3}\kappa^2f^{3/2} + \frac{4}{7}(G\sigma)^2f^{-1/2}\right)$$

- PBH and WH exhibit distinct frequency dependencies, resulting in different dependencies on the size of the domain wall.

Generation of SGWB

- The generated SGWB:

$$\Omega_{\text{GW}}(f) = \frac{8\pi\sqrt{2}\Omega_r^{1/4}}{3C_2H_0^{3/2}}\Gamma_s\left(\frac{1}{3}\kappa^2f^{3/2} + \frac{4}{7}(G\sigma)^2f^{-1/2}\right)$$

- PBH and WH exhibit distinct frequency dependencies, resulting in different dependencies on the size of the domain wall.
- The turning point of frequency corresponds to the location at where the ALP model can provide the largest size of PBH, i.e.

$$f_{\text{peak}} = \sqrt{8f_a\Lambda^2/(M_{\text{Pl}}^2t_0)}.$$

Generation of SGWB

- The generated SGWB:

$$\Omega_{\text{GW}}(f) = \frac{8\pi\sqrt{2}\Omega_r^{1/4}}{3C_2H_0^{3/2}}\Gamma_s\left(\frac{1}{3}\kappa^2f^{3/2} + \frac{4}{7}(G\sigma)^2f^{-1/2}\right)$$

- Casted in a power-law on experiments:

Generation of SGWB

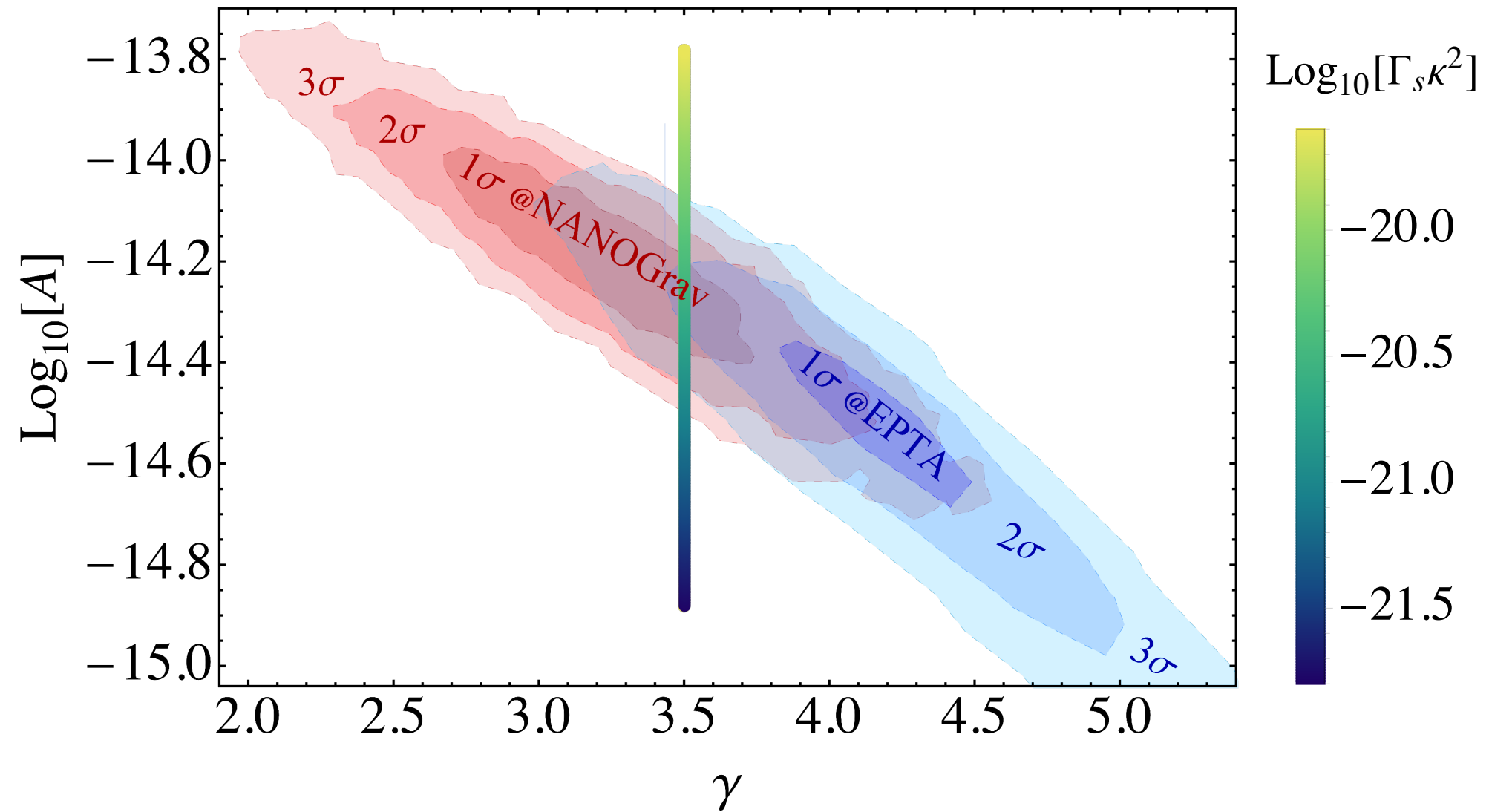
- The generated SGWB:

$$\Omega_{\text{GW}}(f) = \frac{8\pi\sqrt{2}\Omega_r^{1/4}}{3C_2H_0^{3/2}}\Gamma_s\left(\frac{1}{3}\kappa^2f^{3/2} + \frac{4}{7}(G\sigma)^2f^{-1/2}\right)$$

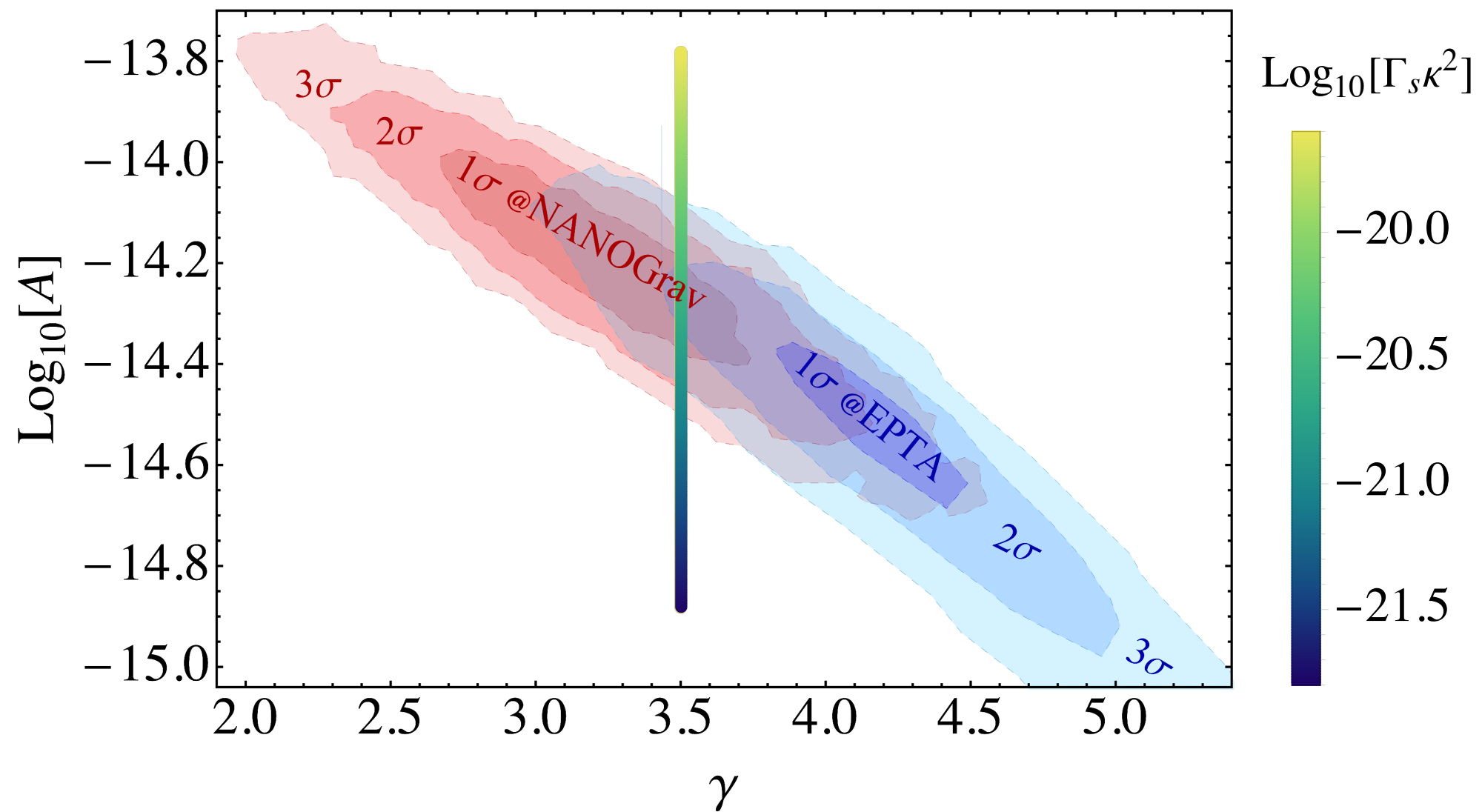
- Casted in a power-law on experiments:

$$\Omega_{\text{GW}}(f) = \frac{2\pi^2}{3H_0^2}f^2h_c(f)^2 = \frac{2\pi^2}{3H_0^2}A^2f_{\text{yr}}^2\left(\frac{f}{f_{\text{yr}}}\right)^{5-\gamma}.$$

Generation of SGWB

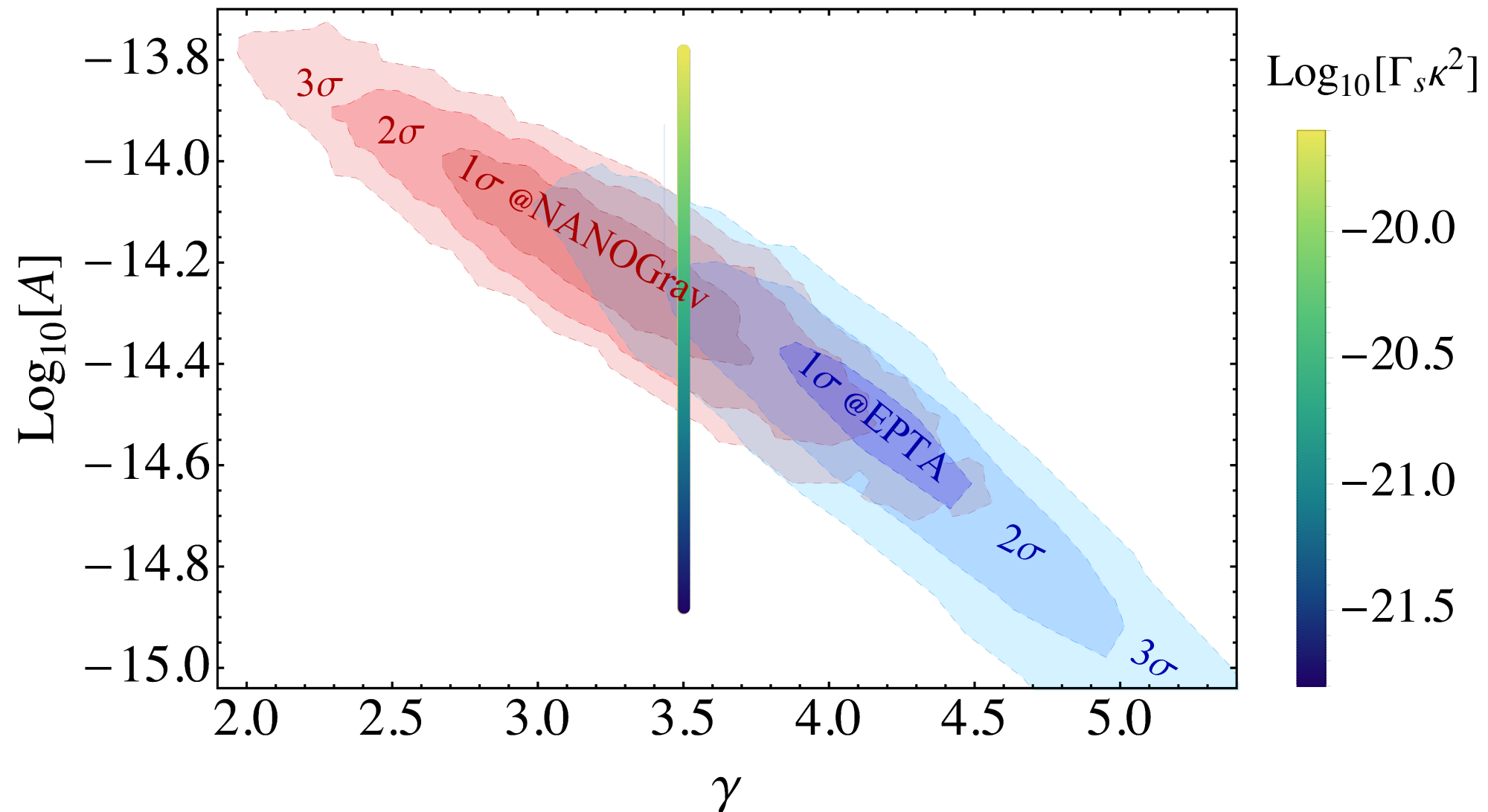


Generation of SGWB



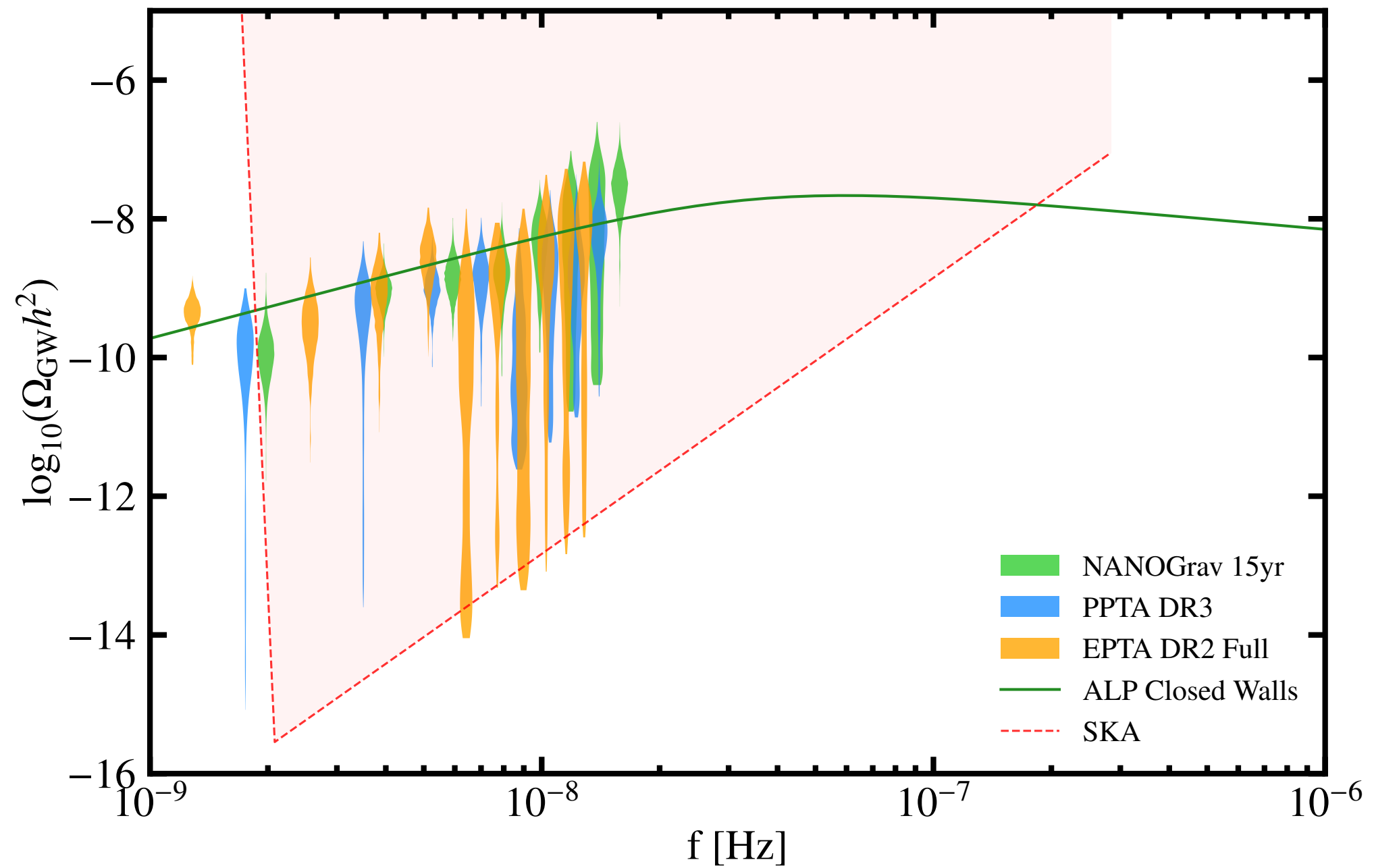
- NANOGrav shows consistent with EPTA in 2σ .

Generation of SGWB

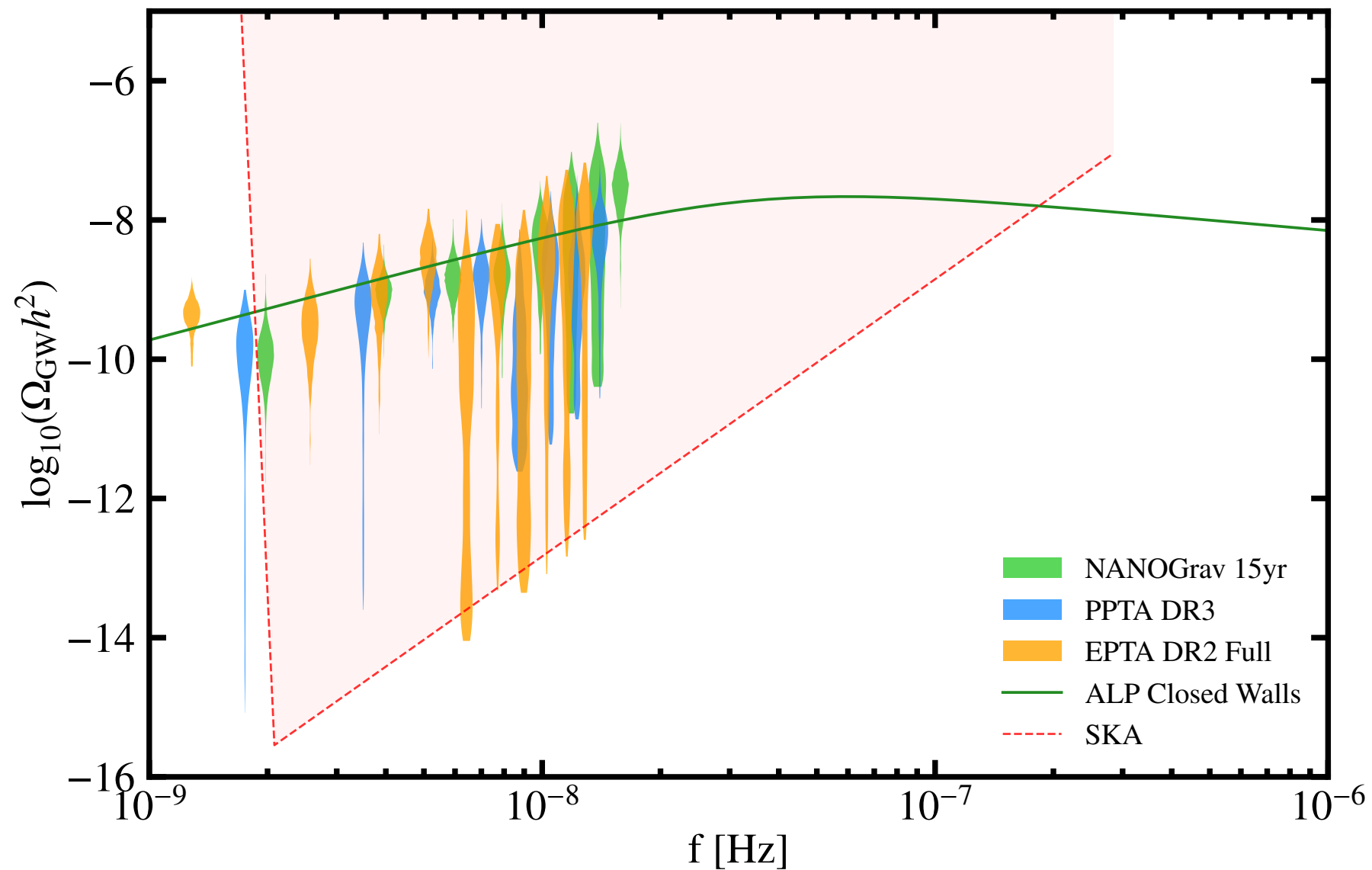


- NANOGrav shows consistent with EPTA in 2σ .
- Ω_{gw} from WH gives $\gamma = 3.5$, while Ω_{gw} from PBH gives $\gamma = 5.5$. Hence domain walls escape into baby universe give a better explanation on PTA data.

Generation of SGWB



Generation of SGWB



- Domain walls escape into baby universe show a compelling explanation for the PTA observations, with $f_{\text{peak}} \geq f_{\text{yr}}$.

Implication on JWST observations

Implication on JWST observations

- The James Webb Space Telescope reported **six** candidate massive galaxies with **stellar mass greater than $10^{10} \odot$** , at high redshift, **$7.4 \leq z \leq 9.1$** .

Implication on JWST observations

- The James Webb Space Telescope reported **six** candidate massive galaxies with **stellar mass greater than $10^{10} \odot$** , at high redshift, **$7.4 \leq z \leq 9.1$** .
- Challenges the current theoretical framework of early structure formation. Stellar mass of a galaxy is constrained by the mass function of dark matter halos.

Implication on JWST observations

- The James Webb Space Telescope reported **six** candidate massive galaxies with **stellar mass greater than $10^{10} \odot$** , at high redshift, **$7.4 \leq z \leq 9.1$** .
- Challenges the current theoretical framework of early structure formation. Stellar mass of a galaxy is constrained by the mass function of dark matter halos.
- Seeds effect of the ALP may modify the power spectrum at small scale, results in cumulative massive stellar mass.

Implication on JWST observations

- Comoving mass density above the threshold, in dark matter halos:

Implication on JWST observations

- Comoving mass density above the threshold, in dark matter halos:

$$\rho(M_{\star} \geq M_{\star}^{\text{obs}}) = f_b \epsilon_{\star} \int_{M_h^{\text{cut}}}^{\infty} M_h \frac{dn(z_{\text{obs}}, M_h)}{dM_h} dM_h$$

Implication on JWST observations

- Comoving mass density above the threshold, in dark matter halos:

$$\rho(M_{\star} \geq M_{\star}^{\text{obs}}) = f_b \epsilon_{\star} \int_{M_h^{\text{cut}}}^{\infty} M_h \frac{dn(z_{\text{obs}}, M_h)}{dM_h} dM_h$$

M_h —halo mass

M_{\star} —stellar mass

Implication on JWST observations

- Comoving mass density above the threshold, in dark matter halos:

$$\rho(M_{\star} \geq M_{\star}^{\text{obs}}) = f_b \epsilon_{\star} \int_{M_h^{\text{cut}}}^{\infty} M_h \frac{dn(z_{\text{obs}}, M_h)}{dM_h} dM_h$$

M_h —halo mass

M_{\star} —stellar mass

f_b —baryon fraction

ϵ_{\star} —star formation efficiency

Implication on JWST observations

- Comoving mass density above the threshold, in dark matter halos:

$$\rho(M_{\star} \geq M_{\star}^{\text{obs}}) = f_b \epsilon_{\star} \int_{M_h^{\text{cut}}}^{\infty} M_h \frac{dn(z_{\text{obs}}, M_h)}{dM_h} dM_h$$

M_h —halo mass

M_{\star} —stellar mass

f_b —baryon fraction

ϵ_{\star} —star formation efficiency

$$M_{\star} = f_b \epsilon_{\star} M_h$$

Implication on JWST observations

- Distribution of the ALP domain walls:

Implication on JWST observations

- Distribution of the ALP domain walls:

$$\frac{dn}{dM} = \frac{\Gamma_s}{2} \frac{1}{t_{\text{eq}}^{3/2}} (4\pi\sigma)^{3/4} M^{-7/4}$$

Implication on JWST observations

- Distribution of the ALP domain walls:

$$\frac{dn}{dM} = \frac{\Gamma_s}{2} \frac{1}{t_{\text{eq}}^{3/2}} (4\pi\sigma)^{3/4} M^{-7/4}$$

Γ_s —domain wall contour formation rate

Implication on JWST observations

- Distribution of the ALP domain walls:

$$\frac{dn}{dM} = \frac{\Gamma_s}{2} \frac{1}{t_{\text{eq}}^{3/2}} (4\pi\sigma)^{3/4} M^{-7/4}$$

Γ_s —domain wall contour formation rate

t_{eq} —time of matter-radiation equality

Implication on JWST observations

- Distribution of the ALP domain walls:

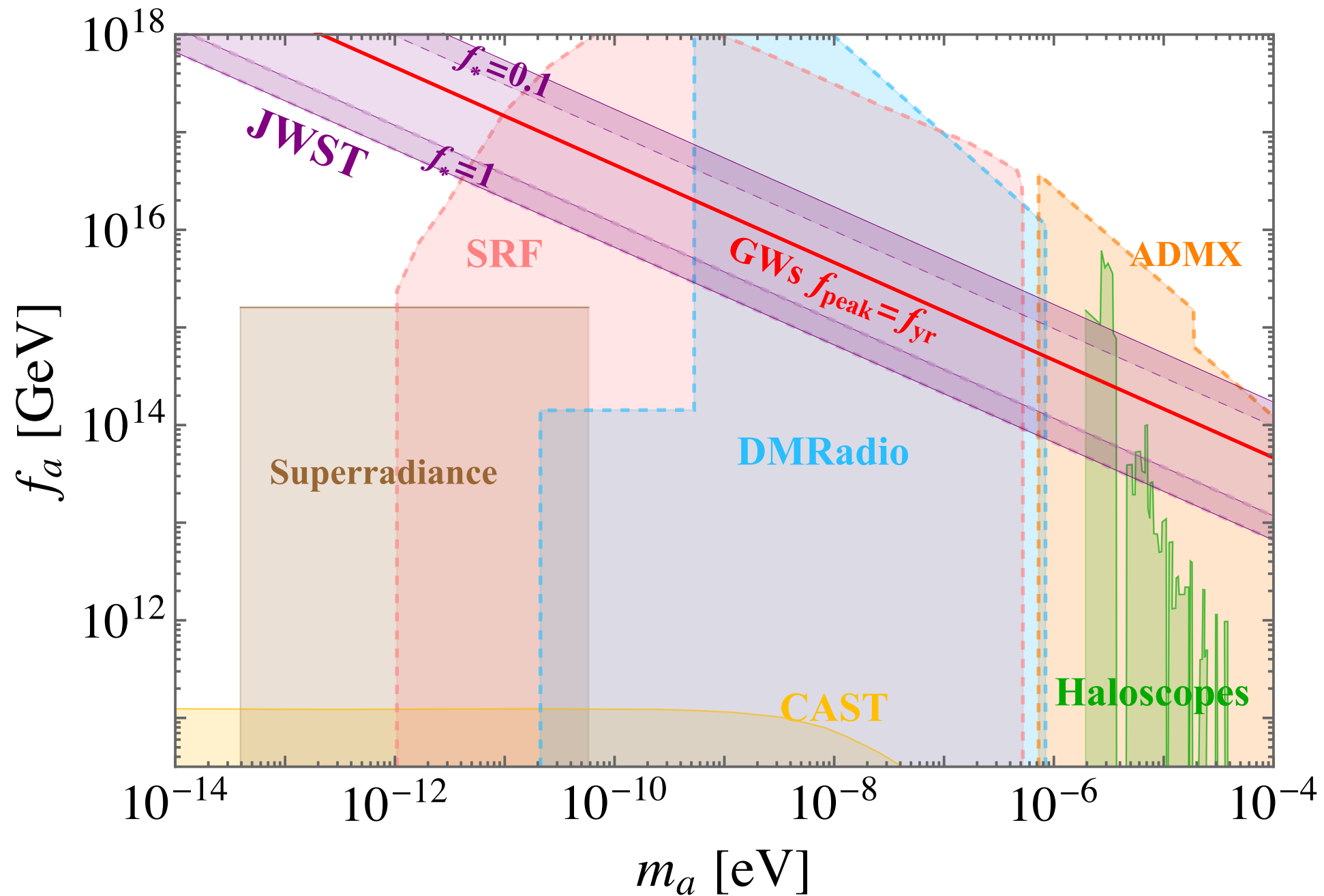
$$\frac{dn}{dM} = \frac{\Gamma_s}{2} \frac{1}{t_{\text{eq}}^{3/2}} (4\pi\sigma)^{3/4} M^{-7/4}$$

Γ_s —domain wall contour formation rate

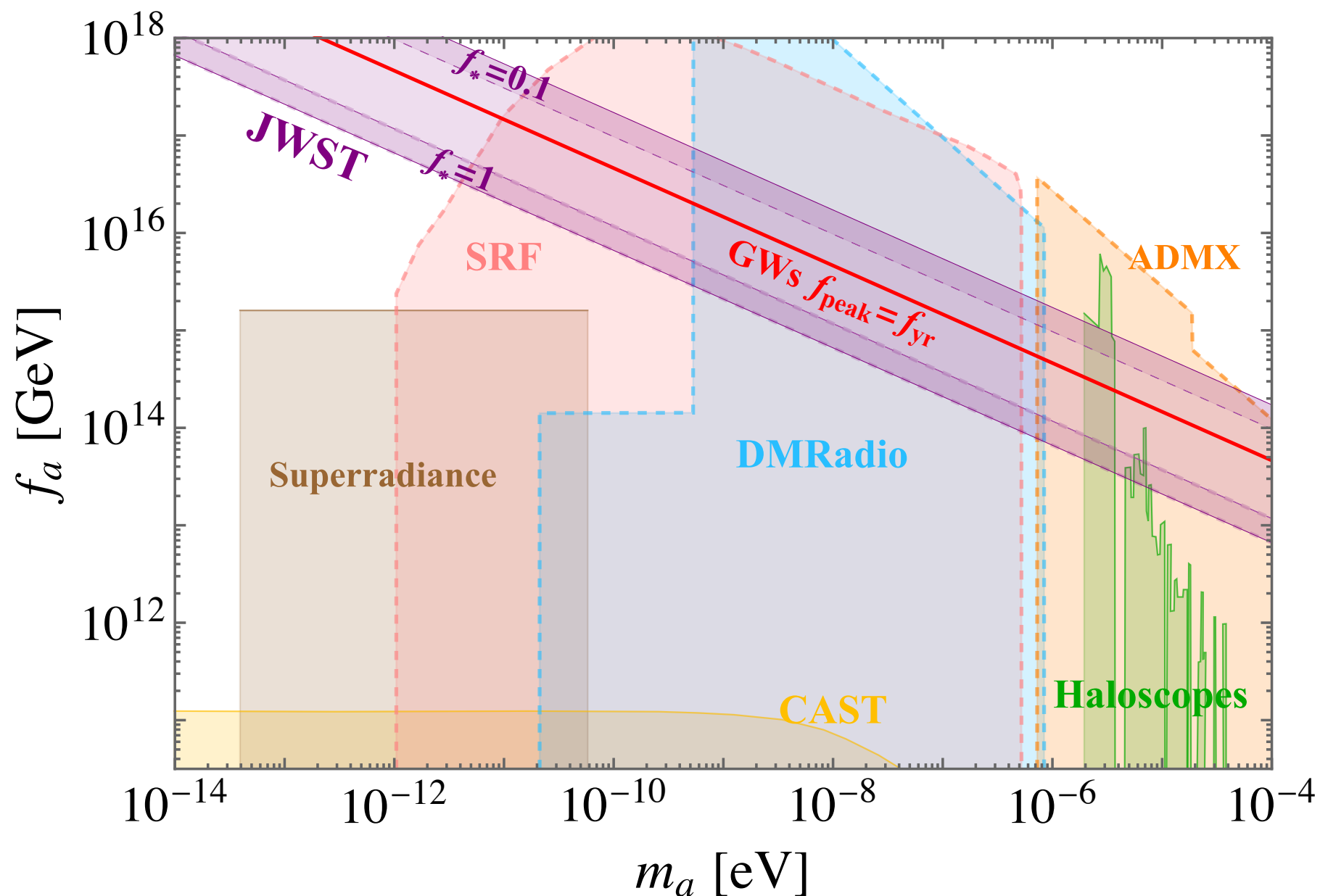
t_{eq} —time of matter-radiation equality

$\sigma(\Lambda, f_a)$ —domain wall tension

Joint constraints from JWST and ALP searching



Joint constraints from JWST and ALP searching



- The (f_a, m_a) , which provide suitable GWs peak frequency, lie in the allowed parameter region to give out the JWST observations. And could be probed by the future axion experiments.

Conclusion

- We explore the characteristics of the SGWB within a typical ALP model. We discover that the domain walls, resulting from ALPs fluctuations during inflation, which escape into baby universes and radiate energy by GW, can effectively account for the recent nano-Hertz SGWB observations.
- Additionally, the initial fluctuations of ALPs play a crucial role in the formation of cosmological structures, giving rise to the massive galaxies observed by JWST. Our findings demonstrate that the ALP parameters capable of explaining PTA data also align with the observations made by JWST. Consequently, we establish a concise framework that encompasses both of these observations.